A pulsed Grimm glow discharge as an atomic emission source

Chenglong Yang, Kristofor Ingeneri and W. W. Harrison*

Department of Chemistry, University of Florida, Gainesville, FL 32611-7200, USA

Received 15th September 1998, Accepted 25th January 1999

JAAS Journal of Analytical Atomic Spectrometry

A high voltage, microsecond regime pulse dc glow discharge was applied to a standard Grimm source on a modified LECO SA-2000 direct reader spectrometer and to a duplicate Grimm source coupled to a scanning monochromator. The effects of experimental conditions, including pulse voltage, pulse frequency, pulse width and Ar pressure, on Cu atomic and ionic emission intensities were examined and compared with continuous discharge results. The pulsed Grimm source has a higher sputtering rate, greater signal intensity and lower detection limits. The pulsed signal for atomic lines shows a different temporal response from ionic lines. Pulsed Grimm GD-AES also offers control features advantageous in the measurement of thin surface layers.

Introduction

The glow discharge (GD) has proven to be a very useful atomic spectroscopy source for the direct analysis of solid samples owing to its numerous advantages, which include the simplicity of the source itself, excellent detection limits (ppb), minimal matrix effects and a broad elemental coverage.[1–3] The Grimm FD[4] is the most widely applied source for atomic emission spectrometry, a technique represented by several commercial instruments. GD-AES using a Grimm source has the advantages of easy sample interchange, good precision, wide dynamic range and relatively small matrix effects. It has the ability to achieve both bulk and depth-resolved elemental analysis. Therefore, it is now a routine tool for the direct elemental analysis of solids.[5]

The Grimm GD has been powered by direct current (dc) and radiofrequency (rf) sources.[6,7] Both modes are routinely operated at power levels of tens of watts. The instantaneous power of the microsecond pulsed GD can routinely reach several hundred watts, and even up to more than 1000 W in some conditions.[8] Pulsed operation of conventional glow discharges and hollow cathode lamps has been shown to enhance sputtering rates and signal intensities by 1–4 orders of magnitude in emission, fluorescence and mass spectrometry.[9,10] The purpose of this study was to extend the investigations of the microsecond pulsed discharge to include its application to the important Grimm source, including certain initial evaluations of critical parameters.

Experimental

Apparatus

A schematic diagram of the microsecond pulsed dc Grimm GD-AES system is shown in Fig. 1. Two spectrometers were used in the experiment. One was a modified (pulsed source and gated detection) multi-channel direct-reading spectrometer, LECO (St. Joseph, MI, USA) SA-2000, which uses a 0.4 m direct-reading spectrometer with a 2400 groove holographic grating. Spectra collection was done with a sequential monochromator [Chromex (Albuquerque, NM, USA) 500IS/SM] equipped with a 1200 grooves mm^{-1} grating. The standard LECO Grimm GD sources have been described in detail elsewhere.[7] In the model used for this study, the tubular-shaped anode of the source extended to approximately 0.2 mm from the sample. The inner diameter of the anode was 4 mm.

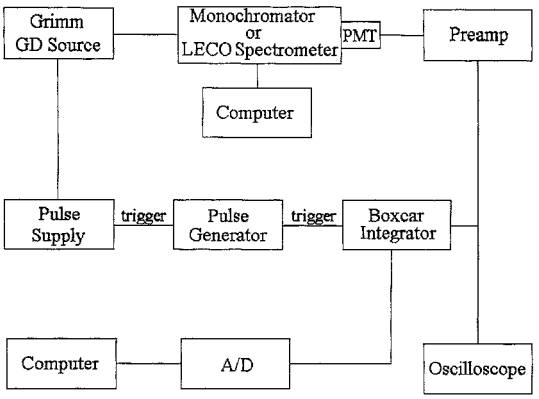

Fig. 1 Schematic diagram of pulsed Grimm GD optical system and gated detection.

The Grimm glow discharge was operated in both the continuous and pulsed modes. In the dc mode a high voltage dc power supply from the LECO SA-2000 system was used. In the pulsed mode, a high voltage pulsed power supply (Model 350, Velonex, Santa Clara, CA, USA) was employed. The pulse width and frequency of the pulsed generator were varied from 0.1 to 300 μs and from 1 to 100 000 Hz, respectively. Voltages up to 3000 V could be applied to the glow discharge source. The pulsed power supply is capable of internally controlled pulsed operation, but a separate waveform generator [Hewlett-Packard (Palo Alto, CA, USA) Model 8003A] was used to trigger both the pulse power supply and the oscilloscope in order to synchronize the discharge and resulting emission signal.

An alternative signal readout and data handling system was used to monitor the microsecond pulsed signal, as the standard SA-2000 system is designed for continuous signals. Output current pulses taken directly from the photomultiplier tubes were converted to pulsed voltage signals by measurement across a 66.3 kΩ resistor. The signals were processed in two ways. The first system consisted of a 2 Gsa s^{-1} (gigasamples per s), 400 MHz, four channel, digital storage oscilloscope (Hewlett-Packard Model 54542C). The output signal, discharge voltage and discharge current were displayed simul-

taneously on the oscilloscope. The voltage was attenuated through a 1000:1 voltage probe, while the discharge current was determined by calculation from the peak voltage dropped across a 5.1 Ω carbon resistor.

The second readout system consisted of a gated boxcar and a computer. The signals from the PMTs were temporally gated and processed with a boxcar integrator (SR250, Stanford Research Systems, Sunnyvale, CA, USA), then the signals from the boxcar were sent to a computer *via* an analog-to-digital (A/D) converter (SR245, Stanford Research Systems). The timing diagram of the system involves a waveform generator to control both the pulsed power supply and the boxcar integrator. A variable delay time (t_d) of 1 ns–10 ms with a variable pulse width (t_w) of 1 ns–15 μs was available in the boxcar integrator. The delay window selected the measurement interval before emission data were taken after initiation of the pulse discharge.

A custom 32-channel gated data system has now been developed and added to the SA-2000, but was not available at the time of this work.

Sample preparation

A pure copper sample (99.9%) and iron standard samples (spectrometric reference materials cast iron C18.8, CKD232–239, Research Institute CKD, Prague, Czech Republic) were used as flat-faced blocks to couple to the Grimm source. Copper films on polished steel substrates were prepared in the Department of Materials Science and Engineering, University of Florida.

Results and discussion

Compared with other GD configurations, which have a significant, but variable cathode and anode distance, the Grimm model depends on an anode that is positioned very close to the cathode, within the dark space distance. In this way, the discharge is confined and the sampled surface area is well defined by the diameter of the anode. This makes the Grimm source particularly advantageous for the study of thin layer samples. Some disadvantages are also encountered with a Grimm source. The sample must be very flat to permit a vacuum seal against an O-ring fitting and to allow a continuous cathode–anode distance around the sampled area. Because this distance is so small, sputtering can produce non-uniform deposition around the crater, effects that may short out the electrodes or cause discharge instabilities, although this was not encountered in these experiments.

In the case of the microsecond pulse discharge, high sputter rates are developed during the discharge on-time, so we were interested in detecting any deleterious effects that might be produced with a Grimm source. In a broader sense, the GD plasma in the Grimm source is confined within a narrow tubular anode, so another aspect of this study was to determine whether high power discharge pulses would exhibit different responses to the more open GD design.

Typical pulse profiles

Fig. 2 shows atomic and ionic emission profiles for two copper lines, relative to the pulse voltage and current waveform as displayed on the oscilloscope. Typically, a 10 μs 2500 V pulse was applied to the Grimm source with 100 Hz operating frequency. At the beginning of the pulse cycle, the current rises sharply within the first microsecond after the voltage application, reaches about 3 A at 2 μs, then with a rapid drop in discharge resistance decreases to a plateau region of 0.5 A at 3 μs and maintains this value for the duration of the pulse. The discharge voltage rises abruptly owing to capacitative

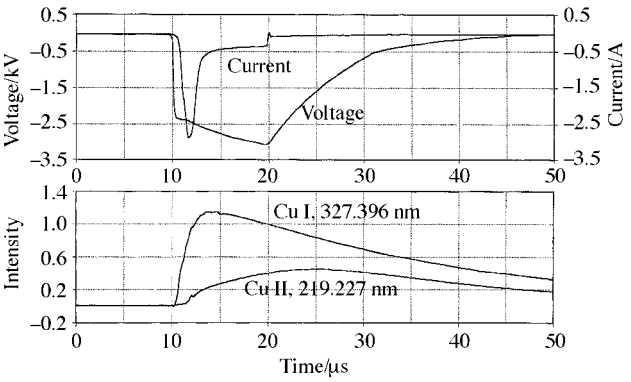

Fig. 2 Typical time-resolved profiles for a pulsed Grimm GD at 100 Hz.

charging of the argon gas and after breakdown continues to rise slowly even to discharge termination.

Applying a high voltage does not immediately yield a copper emission signal, which appears only after the current builds and sufficient sputtering has taken place (~1 μs after initiation). At that point, the sputter injection of copper atoms causes Cu I emission to increase sharply with current, peaking around the 3 μs point, then decreasing slowly over the remainder of the pulse. The emission remains high even after the current has dropped to its plateau value owing to the slow diffusion rate of the sputtered atoms and the presence of metastable Ar atoms to sustain excitation at high levels.

Because of the emission intensity available from a microsecond pulsed discharge, the response of the elemental ions is of interest, as these species are enhanced greatly compared with the case of dc discharges.[8] We are also interested in ions for their direct role in GD mass spectrometry.[11] In the case of copper (but not with all elements[12]), ion emission lags behind that from atoms. As shown in Fig. 2, the Cu II emission exhibits a brief delay before its appearance and then increases gradually to a maximum around 15 μs, which is 10–12 μs later than the maximum for Cu I. The mechanism for this response is not clear, although it could be related to the timing of maximum argon metastable formation and the well known related ionization step.[13] In any case, the timing delay set for optimum signal acquisition for elemental emission will be a function of the species measured. In some cases, there could be an advantage in selecting an intense ion line and setting a delay time that provides temporal discrimination against potentially interfering atomic lines.

Electrical characteristics of pulsed Grimm GD

The analytical performance of a GD source is closely related to its electrical properties. While the standard operating characteristics of a Grimm source are well known, it was important to determine how the Grimm source responded to the high voltage, high current pulses over a range of conditions. The relationship between discharge current and voltage at a given source pressure provides the most fundamental display of GD characteristics. Normally, the discharge of a Grimm lamp is self-sustaining and operates in an abnormal region. Therefore, increases in discharge current must be accompanied by increases in operating voltage at a constant pressure. Fig. 3(a) indicates that this is true for the pulsed operation, showing a plot of the peak pulse voltage of the GD source as a function of peak current for two different pressure regimes, 3 and 4.5 Torr argon. A linear relationship is observed at each pressure, which implies a similar response of power with increased current, and likewise of sputtering rate. It can also be seen in Fig. 3(b) that the two pressures create different plasma impedances as the power levels increase. Peak powers

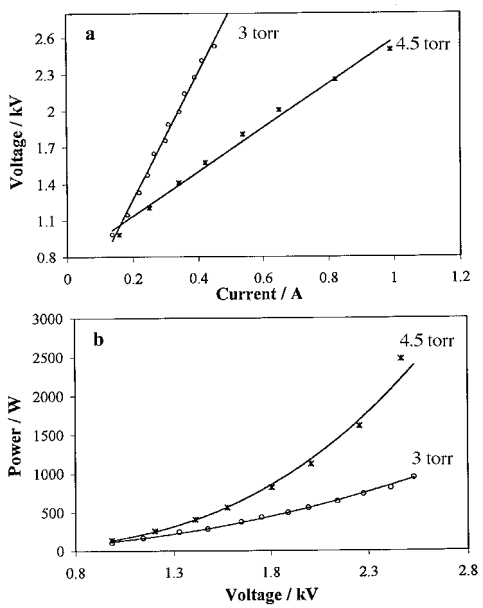

Fig. 3 Electrical characteristics for pulsed Grimm GD lamp at 3 and 4.5 Torr Ar using a Cu cathode. (a) Voltage *versus* current; (b) power *versus* voltage.

of 2–3 kW are attained for the 10 μs pulse, compared with typical continuous power levels of 60 W for the dc mode. It is significant that the usual pulse operating conditions produce a discharge in which the average power is lower than that of the dc mode because of the reduced duty cycle. Pulse frequency and pulse width determine the average power delivered to the discharge. Normally, with a Cu cathode, the peak power is 750 W with a pulse of 2000 V, 100 Hz frequency, 10 μs pulse width and 3 Torr pressure. However, the average power is only 0.56 W, so the cooling system required for normal Grimm GD operation is not necessary in the pulse mode.

Optimization of operating parameters

Studies on the effect of pulse operating voltage, pulse width, pulse frequency and support gas pressure on copper atomic and ionic emission intensity were carried out using a pure Cu sample. The emission response from Cu I (327.396 nm) and Cu II (219.226 nm) was monitored as a function of pulse voltage and current. Compared with the standard dc discharge, the pulse discharge would be expected to produce enhanced emission intensities, which is indeed the case, as will be shown in a later section. The pulse discharge exhibits a disproportionate enhancement of ion emission over that from neutral atoms, particularly as the pressure and related power of the pulse increase. Fig. 4 shows the effect of increasing pressure on Cu II and Cu I intensities, both of which increase with pressure, but the ion signal rises more rapidly. At low pressures (and thus low powers) the ion line shows no special prominence, but as power is increased the ion signal intensity approaches that of the atom signal. Bogaerts and Gijbels[14] suggested that under high power conditions, asymmetric charge transfer may become a dominant ionization process in comparison with Penning ionization, producing more efficient ionization. The practical significance of this effect is to make certain ion lines sufficiently intense as to be analytically viable alternatives in cases where spectral interferences may preclude the use of neutral atom lines. The emission spectrum of a pulsed GD shows many more prominent ion lines.

In principle, the use of extended pulse widths beyond the standard 10 μs should increase the discharge duty cycle accordingly and produce a linear increase in power and net sputtering. In practice, this is not observed. As shown in Fig. 2, the peak

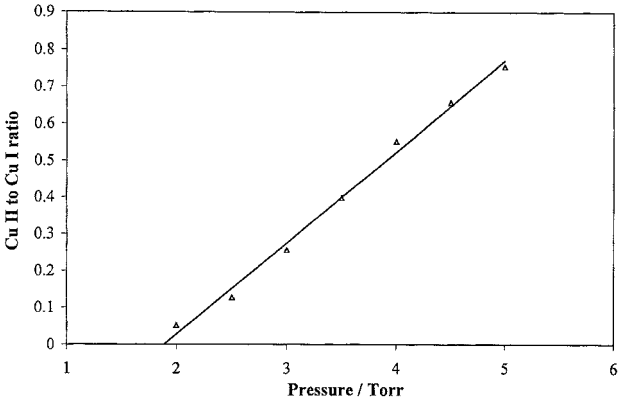

Fig. 4 Effect of discharge pressure on Cu II-to-Cu I ratio at 2000 V, 10 μs and 50 Hz pulse. Cu I, 327.39 nm; Cu II, 219.23 nm.

current response takes the form of a sharp initial pulse, followed by rapid decay to a lower power (resistance) level. The response is probably also affected by the power supply being unable to sustain the high peak currents. In any case, wider pulses have limited advantage in that the low current plateau is extended, but with a decrease in the initial peak current amplitude. The effect of pulse width is shown for copper ion emission in Fig. 5. Longer pulses decrease the peak emission while adding only marginally to the temporal response, so that no analytical advantage is gained. A 10 μs pulse provides the optimum response in balancing emission, power and stability. No significant effect from frequency variation was observed.

Comparison of emission and sputtering rates

The peak power of the pulsed Grimm GD is considerably higher than the steady-state level from the dc Grimm GD, resulting in higher short term intensity and sample sputtering. A direct comparison of the emission signals, with each source operating at its normal conditions, is shown in Fig. 6 for Cu I and Cu II. A data gate set to sample each discharge at its maximum intensity shows that the Cu I and Cu II intensities increased by factors of 15 and 16, respectively. The net advantage includes the ability to operate at low average power while still obtaining higher peak emission.

Operating a GD at high peak power implies enhanced sputter rates during the pulse period, both from an increased number of sputtering ions striking the cathode and also from the fact that the average energy of the impacting ions is higher, which increases the sputter yield. The pulsed nature of the

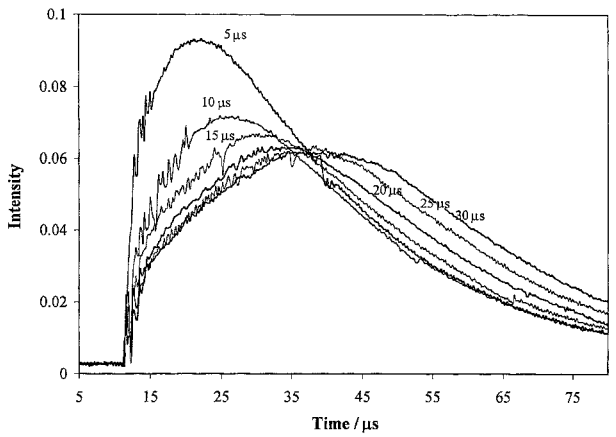

Fig. 5 Effect of pulse width on Cu II emission at 2000 V pulse with operating frequency of 50 Hz and 3 Torr Ar. Cu II, 219.23 nm.

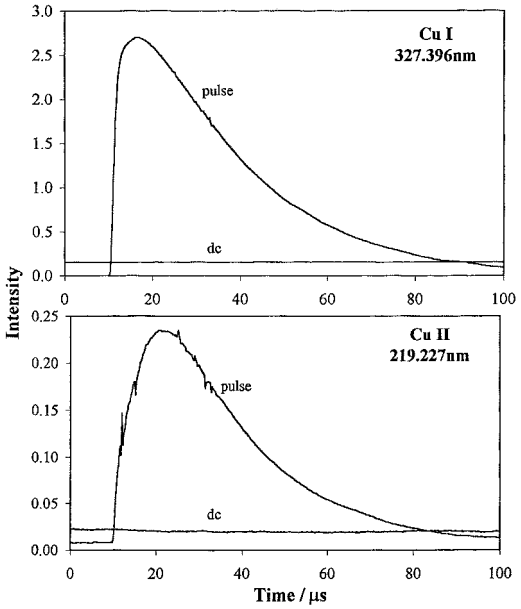

Fig. 6 Comparison of Cu I and Cu II emission profiles from dc and pulsed Grimm GD-AES. Pulse: 2500 V, 972 W (peak), 0.49 W (average) and 3.5 Torr Ar. Dc: 1200 V, 38 W and 5 Torr Ar.

discharge permits controlled erosion of a surface by variation of the pulse frequency. We carried out direct mass loss measurement for sputtering rates with both types of discharge. The net sputter rate of a continuous discharge is greater than with this pulsed dc, but during the measurement time of the microsecond discharge, much higher sputtering rates occur. A 10 μs 2000 V pulse at 3 Torr pressure at 422 W peak power, but only 0.42 W average power, removes about 2000 Å of a Cu disk (4 mm effective surface diameter) per minute with a pulse frequency of 100 Hz. From this, the net sputtering rate is about 3.5×10^{13} atoms per pulse. In the dc mode at 1200 V, 5 Torr pressure and 37 W continuous power, a 132 000 Å min^{-1} removal rate is measured. If we calculate then on comparable time-scales, the net sputtering rate of the dc discharge in a 10 μs interval is roughly 2.5×10^{12} atoms. On this basis, the sputtering rate of a pulsed Grimm GD is enhanced about 14 times compared with that of dc Grimm GD during the pulse cycle. However, since the on-time is very short and each pulse is reproducible within about 5%, careful control of the surface removal process is possible by adjustment of pulse frequency.

It is also important to note that we have not experienced any problems with sputter deposition of cathode material relative to shorting out the cathode–anode gap. Craters formed have been symmetrical with smooth edges. Even after several hours of discharge time, no instability has been observed.

Thin-layer sample analysis

The Grimm GD has proven to be an excellent tool for depth profile analysis,[7] using both dc and rf discharges. The applications have tended to be comparatively thick layers in the micrometer range, such as metal or alloy protective coatings. Limitations for GD thin layer analysis include possible uneven crater formation and also atomic mixing due to redeposition of sputtered atoms back on to the surface, caused by collisions with discharge gases. High vacuum techniques such as SIMS avoid some of the problems found with a GD, although it is not without its own limitations. The minimal matrix effects in GD analysis promote efforts to extend the GD to thin film analysis.[15]

The microsecond pulsed discharge allows short term, repetitive stripping of atoms from a thin film. Layers of only a few atomic distances can be removed during the period of several hundred pulses extending over as much time as the pulse frequency determines. There is therefore sufficient time to stabilize the discharge and collect depth profile data, whereas with a continuous discharge a very thin film may be removed in seconds. The pulsed nature of the discharge may also reduce somewhat redeposition from collision with other sputtered atoms due to the removal of these atoms between pulses.

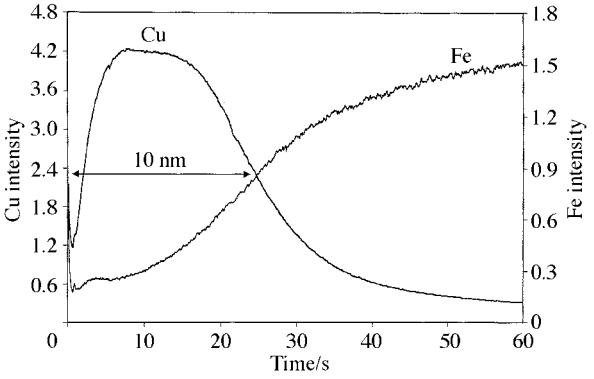

Fig. 7 Depth profile of a 10 nm Cu film deposited on steel. Conditions: 1000 V, 10 μs, 200 Hz pulse and 4 Torr Ar. Cu I, 327.39 nm; Fe I, 327.99 nm.

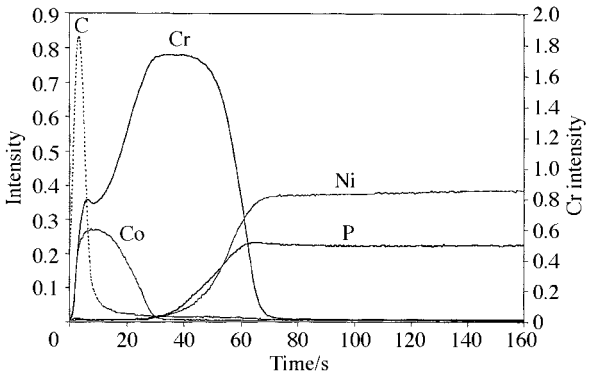

Fig. 8 Depth profile of a computer hard-disk. Conditions: 1200 V, 10 μs, 600 Hz pulse and 4 Torr Ar. C I, 165.70 nm; Cr I, 425.43 nm, Co I, 345.35 nm; Ni I, 349.30 nm; P I, 178.29 nm.

Fig. 7 shows the removal of a 10 nm deposited copper layer from a steel substrate. The uniformity of both the deposited film and the base material was not optimum, but the results showed that layers of this magnitude could be removed with about 5% reproducibility (three trials), as determined from the total time to the crossing point of the plots. Thin film standard samples were not available to us, but we did examine a well known sample type that contains multiple thin layers, namely magnetic disc hard drives taken from spent computers. Fig. 8 shows results taken from an IBM computer hard drive, indicating that the pulsed GD method can resolve and identify the several disk layers. Manufacturers of these disks do not make readily available details of construction and composition for comparison with our results. The advantage of the application of Grimm GD to such samples is the complete lack of preparation time required. The disks are simply placed against the source O-ring mount and analyzed directly.

Cu emission spectra

Previous work in our laboratories has achieved a beneficial separation of the signal from background in pulsed GD time-of-flight mass spectrometry.[16] Similarly, work with the pulsed GD hollow cathode lamp has shown some interesting temporal

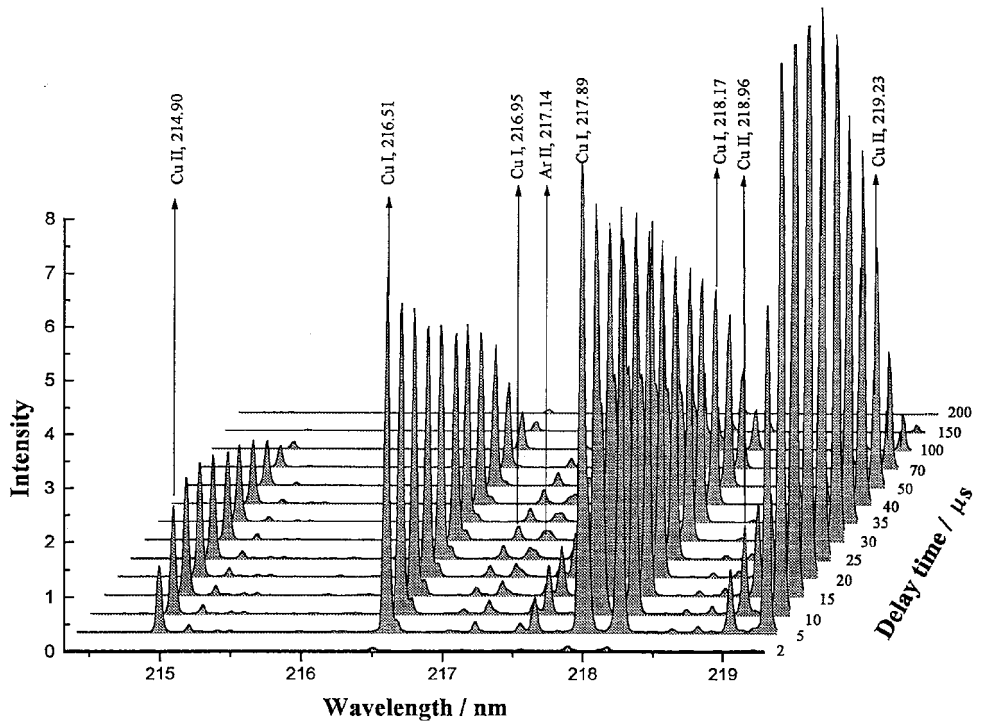

Fig. 9 Time-resolved spectra from a pulsed Grimm GD lamp (Cu sample) at 2000 V, 10 μs, 600 Hz pulse and 3 Torr Ar.

separation among various plasma species.[11] Fig. 9 shows the results of a comparable study with the pulsed Grimm source by delaying the gate time after discharge initiation. Even at the initial delay time of 2 μs, a signal for Cu I is observed, but no Cu II emission is present. The Cu I emission reaches its maximum at a delay time of 5 μs. However, Cu II emission forms later and maximizes at about 15 μs. Temporal responses from the pulsed signal for several other elements were also measured and are presented later. In principle, by optimizing the time delays appropriately for specific elemental lines, better analytical signals can be obtained, particularly for ion lines *vs.* atom lines.

Different temporal response for atomic and ionic lines

Examples of different temporal responses for atomic and ionic lines of four elements (all at 2000 V, 10 μs, 50 Hz pulse and 3 Torr pressure) are shown in Fig. 10. In the case of each element, the sputtered atom emission appears earlier than the ionic emission. The atomic lines reach a maximum during the duration of the pulse, but the ionic lines contrast by maximizing

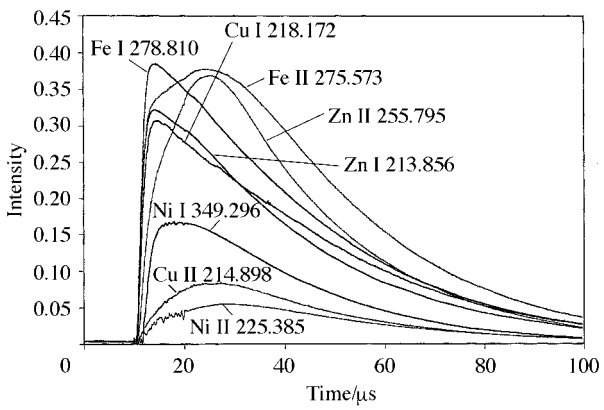

Fig. 10 Temporal elemental emission profiles of pulsed Grimm GD at 2000 V, 10 μs, 50 Hz pulse and 3 Torr Ar.

only a few microseconds after pulse termination. Both types of emission depend on sputter ablation of the cathode atoms, with subsequent collisional effects in the GD plasma to cause excitation. The time-scale we see here seems much too slow to be attributed to any fundamental stepwise ionization process. More likely is some discharge termination effect that creates electrons or other species more optimal for ionization (*e.g.*, charge transfer possibilities). Recall, of course, that we are not observing actual atom or ion populations as such; we see instead that fraction excited. We can only suggest at this point that there are different temporal responses of atoms *vs.* ions for these particular elements.

Analytical characteristics of the pulsed Grimm source

For potential utility of a pulsed Grimm GD, we should be interested in the source stability, sensitivity and analytical response. The stability characteristics of pulsed Grimm GD-AES were evaluated in terms of a relative standard deviation (RSD) of about 5% for 10 consecutive pulsed signals, as shown in Fig. 11. Obviously, signal averaging would be used in real analytical situations (data taken over a longer period of 1 min, as evidenced in Fig. 8 for nickel and phosphorus, yield RSDs near 1%), but we wished to determine the reproducibility of the raw pulses. In these measurements, the pulse width was reduced to 5 μs to achieve more intense pulse conditions. A standard material (CKD238) containing Cu at 0.92% served as the sample, with pulse conditions of 2500 V, 50 Hz, 5 μs and 2.5 Torr pressure. The RSDs for Cu I and Cu II for peak areas of single pulses are 4.5 and 9.2%, respectively. With signal averaging, better RSDs result. By averaging 64 pulses (slightly over 1 s in time of 50 Hz), RSDs of 1.0 and 2.5% were obtained for Cu I and Cu II, respectively.

Calibration curves were obtained for copper in a range of CKD standard samples, as shown in Fig. 12. Standard conditions employed were 2000 V pulses at 50 Hz, 5 μs pulse width and 3 Torr pressure. Data were obtained for both an atom line and an ion line, with good linearity for each. The regression coefficients for Cu I and Cu II are both 0.996. One hundred pulses at 100 Hz were sampled for each measurement using a

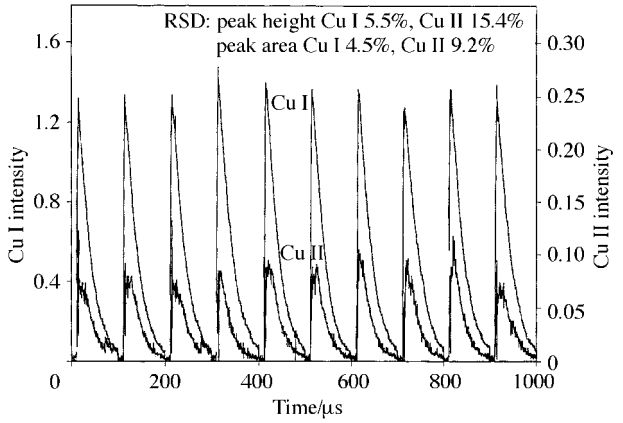

Fig. 11 Single pulse stability comparison of copper atom and ion emission using a CKD238 standard sample (0.92% Cu) at 2500 V, 50 Hz, 5 μs pulse and 2.5 Torr Ar. Cu I, 327.29 nm; Cu II, 219.23 nm.

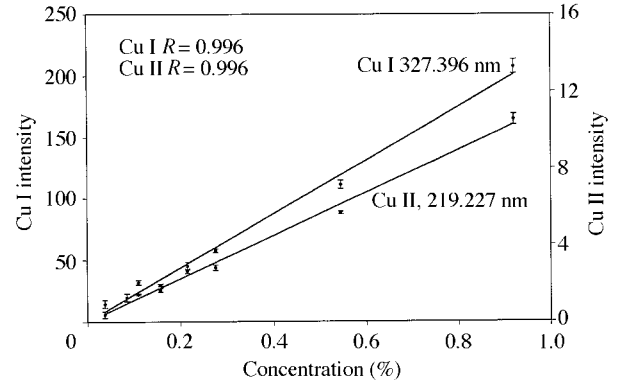

Fig. 12 Calibration curves for Cu in CKD standard samples (atom and ion lines at 2000 V, 5 μs, 100 Hz pulse and 3 Torr Ar.

2.5 μs sampling window. Error bars show the RSD of three sample runs, each at different sample locations, requiring breaking of the sample vacuum between each measurement.

The composition of detection limits for the pulsed discharge *vs.* dc operation is of interest, but we are constrained by our present data system, so only relative indications are justified. Although the signal intensities of most elements in pulsed Grimm GD-AES are enhanced more than 10-fold compared with the dc Grimm GD-AES, the background emission in the pulsed Grimm GD also increases. Therefore, DLs ($3\times$ RSD) for the pulsed mode improve by a factor of $\sim$2–8, dependent upon the line and background response.

Conclusions

The pulsed operation of a Grimm GD shows several interesting analytical advantages, including enhanced sputtering rate and emission intensity compared with the dc mode. The pulsed method also permits more control over sample removal rate, which may be advantageous in the analysis of thin layer samples. The electrical characteristics of a pulsed Grimm GD and the different temporal responses for atomic and ionic lines offer opportunities to elicit a deeper understanding of the discharge mechanism. In order to extract the full potential from the pulsed Grimm GD, a suitable signal accumulation system is required to handle the fast microsecond pulse emission. Based on the results obtained in these optical emission studies, we now plan to modify the source suitably for interfacing with our time-of-flight mass spectrometer to gain complementary information.

Acknowledgements

The authors express their gratitude for the support of this research by the Department of Energy, Basic Energy Sciences and by the LECO Corporation. Also acknowledged are valuable discussions with Drs. Ben Smith and Jim Winefordner.

References

1 *Glow Discharge Spectroscopies*, ed. R. K. Marcus, Plenum Press, New York, 1993.
2 W. W. Harrison, C. M. Barshick, J. A. Klingler, P. H. Ratliff and Y. Mei, *Anal. Chem.*, 1990, **62**, 943.
3 J. A. C. Broekaert, *J. Anal. At. Spectrom.*, 1987, **2**, 537.
4 B. N. Chapman, *Glow Discharge Processes*, Wiley, New York, 1980.
5 A. Bengtson, *J. Anal. At. Spectrom.*, 1996, **11**, 829.
6 K. Wagatsuma and S. Suzuki, *Fresenius' J. Anal. Chem.*, 1997, **358**, 581.
7 A. Bengtson, *Spectrochim. Acta, Part B*, 1994, **49**, 411.
8 X. M. Yan, W. Hang, B. W. Smith, J. D. Winefordner and W. W. Harrison, *J. Anal. At. Spectrom.*, 1998, **13**, 1033.
9 W. Hang, W. O. Walden and W. W. Harrison, *Anal. Chem.*, 1996, **68**, 1148.
10 W. O. Walden, W. Hang, B. W. Smith, J. D. Winefordner and W. W. Harrison, *Fresenius' J. Anal. Chem.*, 1996, **355**, 442.
11 W. W. Harrison, W. Hang, X. Yan, J. Ingeneri and C. Schilling, *J. Anal. At. Spectrom.*, 1997, **12**, 891.
12 C. Yang and W. W. Harrison, in preparation.
13 E. B. M. Steers and F. Leis, *J. Anal. At. Spectrom.*, 1989, **4**, 199.
14 A. Bogaerts and R. Gijbels, *Anal. Chem.*, 1997, **69**, 721A.
15 K. Wetzig, S. Baunack, V. Hoffmann, S. Oswald and F. Praessler, *Fresenius' J. Anal. Chem.*, 1997, **358**, 25.
16 W. W. Harrison and W. Hang, *J. Anal. At. Spectrom.*, 1996, **11**, 835.

Paper 8/07204C